

Impact of Furan Substitution on the Optoelectronic Properties of Biphenyl/Thiophene Derivatives for Light-Emitting Transistors

Periyasamy Angamuthu Praveen,* Perumal Muthuraja, Purushothaman Gopinath, and Thangavel Kanagasekaran*



Cite This: *J. Phys. Chem. A* 2022, 126, 600–607



Read Online

ACCESS |

Metrics & More

Article Recommendations

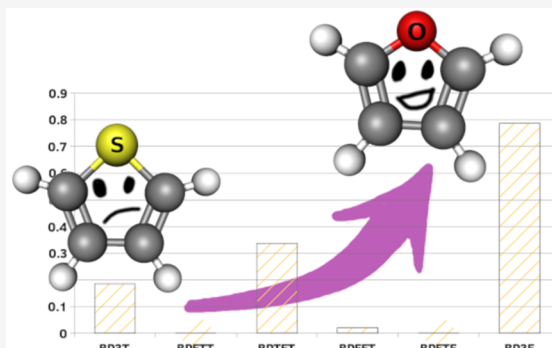
Supporting Information

ABSTRACT: Biphenyl/thiophene systems are known for their ambipolar behavior and good optical emissivity. However, often these systems alone are not enough to fabricate the commercial-grade light-emitting devices. In particular, our recent experimental and theoretical analyses on the three-ring-constituting thiophenes end capped with biphenyl have shown good electrical properties but lack of good optical properties. From a materials science perspective, one way to improve the properties is to modify their structure and integrate it with additional moieties. In recent years, furan moieties have proven to be a potential substitution for thiophene to improve the organic semiconductive materials properties. In the present work, we systematically substituted different proportions of furan rings in the biphenyl/thiophene core and studied their optoelectronic properties, aiming toward organic light-emitting transistor applications. We have found that the molecular planarity plays a vital role on the optoelectronic properties of the system. The lower electronegativity of the O atom offers better optical properties in the furan-substituted systems. Further, the furan substitution significantly affects the molecular planarity, which in turn affects the system mobility. As a result, we observed drastic changes in the optoelectronic properties of two furan-substituted systems. Interestingly, addition of furan has reduced the electron mobility by one fold compared to the pristine thiophene-based derivative. Such a variation is interpreted to be due to the low average electronic coupling in furan systems. Overall, systems with all furan and one ring of furan in the center end capped with thiophene have shown better optoelectronic properties. This molecular architecture favors more planarity in the system with good electrical properties and transition dipole moments, which would both play a vital role in the construction of an organic light-emitting transistor.

1. INTRODUCTION

Organic π -conjugated semiconducting systems are of great interest due to their tunable charge transfer property, which can be utilized in technologically important areas such as organic photovoltaics (OPVs), organic light-emitting diodes (OLEDs), organic field effect transistors (OFETs), and sensors.^{1–3} Even though these carbon-based systems have lower durability than their inorganic counterparts, their tunable structure–property nature along with the flexibility, cost effectiveness, and ease of fabrication made these materials as the ideal candidates for future technological endeavors. In fact, successful commercialization of OLEDs indicates the potentiality of research in related regimes.^{4–6}

From a structural point of view, rigid planar molecules such as acenes are often considered for semiconducting devices due to their excellent charge carrier transport and mobility. This is due to the fact that the rigidity and planarity give rise to close crystal packing and thus reduce the reorganization energy and improve the charge transfer integrals.^{7–9} On the other hand, the close packing leads to strong aggregation of transition



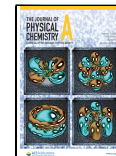
dipole moments (TDM) in the system, resulting in photoluminescence quenching. Thus, better electrical or optical properties of an organic system is often the trade-off.^{10–13} However, considering devices like organic light-emitting transistors (OLET) or long-sought organic lasers, high electrical and optical properties are required. Thus, often systems with high mobility and good PLQY are considered for such requirements.^{14,15}

Thiophene/phenylene derivatives have good mobility and high photoluminescence yield. In particular, due to its synthetic flexibility and strong polarizability, thiophene has received much attention for the development of optoelectronic devices for over a decade.^{16,17} The presence of sulfur atoms in

Received: November 22, 2021

Revised: January 5, 2022

Published: January 20, 2022



thiophene's core gives rise to a strong intermolecular interaction and yields excellent charge carrier mobility. A result, a large number of reports are available on these derivatives for a multitude of applications ranging from OFETS to OPVs.^{18–20}

In the past few years, our group has reported the experimental and theoretical analyses of these thiophene/phenylene-based derivatives toward OLET applications.^{21–23} Our recent theoretical analysis indicated that two derivatives, 5,5''-bis(4-biphenyl)-2,2':5',2"-terthiophene (BP3T) and 2,5-bis(4-biphenyl) tetrathiophene (BP4T), have potential optoelectronic properties.²⁴ BP3T has excellent electronic properties, whereas BP4T has good emissive properties. Our current research focused on these two systems and, in particular, on improving the optical properties in the case of BP3T.

In this regard, we report on the furan-substituted BP3T in the context of being an active medium for OLET devices.²⁵ Furan is an analogous structure to thiophene but with different physical and chemical properties. Due to their large electronegativity and weak intermolecular interactions, for long time these moieties were believed to not be suitable for organic electronic applications. However, recent reports have dispelled such misconceptions and showed excellent charge-transporting behavior in furan systems.^{26,27} Introduction of furan in a π conjugate would result in small torsional angles due to the small atomic size of oxygen. Such a reduction would improve the molecular planarity, crystal packing, and overall charge transport in the system. Further, due to the size of the oxygen atom, furan does not suffer from the heavy atom effect, an effect usually observed in thiophene-based luminescent systems.²⁸ Thus, furans are expected to have a higher photoluminescence yield than their structural counterpart thiophene.

On the basis of these facts, in the present work, we substituted different proportions of furan in the BP3T system in place of thiophene and studied the structural, electronic, and optical properties. Since charge transfer in the system heavily relies on the molecular planarity and rigidity, we focused on these two properties and correlated them to the system's optoelectronic properties.

2. METHODOLOGY

The general molecular structure (BPFT) of the systems studied in this work is given in Figure 1. The furans are substituted in a left to right fashion, replacing thiophenes on each modification. There are two special cases where the center ring is accompanied by their counterparts on either side.

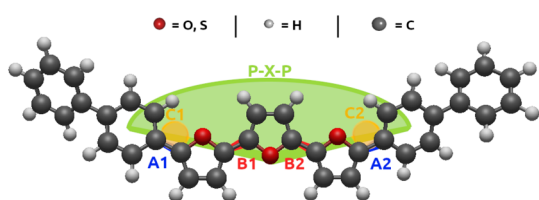


Figure 1. Molecular structure of the BPFT system. A1 and A2 are bond lengths between the phenylene and the thiophene/furan rings. B1 and B2 are bond lengths between the thiophene/furan rings. C1 and C2 are bond angles between the phenylene and the thiophene/furan rings. P–X–P is the dihedral angle with respect to the central ring.

Each obtained geometry along with their IUPAC name is given in Table 1. These geometries were optimized using density functional theory (DFT) calculations. The B3LYP functional with the 6-311G(d,p) basis set was used for the calculations.

After geometry optimization, the nature of the stationary points was evaluated using vibrational frequencies. In the case of ionic states, a spin-unrestricted formalism and time-dependent DFT for the excited states have been used. For the simulation of the charge transfer properties, we used the hopping model. According to Einstein's relation, the mobility of an organic semiconductor at a particular temperature can be estimated by²⁹

$$\mu = \frac{e}{k_B T} D \quad (1)$$

where, μ is the mobility of the organic semiconductor, e is the electronic charge, k_B is the Boltzmann constant, T is the temperature, and D is the diffusion coefficient given by

$$D = \frac{1}{2n} \sum_i r_i^2 W_i P_i \quad (2)$$

where P_i is the hopping probability and r_i is the hopping distance.

For the i th-specific hopping pathway, P_i can be written as

$$P_i = \frac{W_i}{\sum_i W_i} \quad (3)$$

where W is equal to

$$W = \frac{V^2}{\hbar} \left(\frac{\pi}{\lambda k_B T} \right)^{1/2} \exp \left(-\frac{\lambda}{4k_B T} \right) \quad (4)$$

By solving the above Marcus–Hush equation, the nonadiabatic electronic hopping rate (W) can be estimated. Here, V is the electronic coupling between the neighboring molecules and λ is the reorganization energy of the organic semiconductor. Since the intermolecular reorganization energies of the organic system are negligible, in the present case, we considered only the intramolecular reorganization energy, which was calculated from

$$\begin{aligned} \lambda_{\text{hole}} &= \lambda_0 + \lambda_+ \\ &= (E_0^*(Q_+) - E_0(Q_0)) + (E_+^*(Q_0) - E_+(Q_+)) \end{aligned} \quad (5)$$

$$\begin{aligned} \lambda_{\text{electron}} &= \lambda_0 + \lambda_- \\ &= (E_0^*(Q_-) - E_0(Q_0)) + (E_-^*(Q_0) - E_-(Q_-)) \end{aligned} \quad (6)$$

where E_0 and E_+^*/E_-^* are the energies of the neutral and cationic/anionic monomers in the optimized neutral geometry Q_0 and E_0^* and E_+/E_- are the energies of the neutral and cationic/anionic monomers in the optimized cationic/anionic geometry Q_+/Q_- .

To calculate the intermolecular electronic coupling V , the following relation was used,

$$V_{ij} = \left| \frac{(J_{ij} - 0.5(e_i + e_j) \cdot S_{ij})}{(1 - S_{ij}^2)} \right| \quad (7)$$

where S_{ij} is the spatial overlap, J_{ij} is the charge transfer integral, and e_i and e_j are the site energies of the donor and acceptor

Table 1. List of Molecular Systems Used in the Study and Their IUPAC Names

Molecule	IUPAC name	Abbreviated as
	5-[{[1,1'-biphenyl]-4-yl}-5'-(5-[{[1,1'-biphenyl]-4-yl}thiophen-2-yl]-2,2'-bithiophene]	BP3T
	2-[{[1,1'-biphenyl]-4-yl}-5-(5-[{[1,1'-biphenyl]-4-yl}-2,2'-bithiophen]-5-yl)furan]	BPFTT
	5-[{[1,1'-biphenyl]-4-yl}-5'-(5-[{[1,1'-biphenyl]-4-yl}thiophen-2-yl]-2,2'-bifuran]	BPFFT
	2,5-bis(5-[{[1,1'-biphenyl]-4-yl}thiophen-2-yl)furan]	BPFTF
	2-[{[1,1'-biphenyl]-4-yl}-5-[5-(5-[{[1,1'-biphenyl]-4-yl}furan-2-yl]thiophen-2-yl)furan]	BPTFT
	5-[{[1,1'-biphenyl]-4-yl}-5'-(5-[{[1,1'-biphenyl]-4-yl}furan-2-yl]-2,2'-bifuran]	BP3F

states, respectively. These values were calculated using the relation

$$e_{i(j)} = \langle \Psi_{i(j)} | H | P \psi_{i(j)} \rangle \quad (8)$$

$$S_{ij} = \langle \Psi_i | P \psi_j \rangle \quad (9)$$

$$J_{ij} = \langle \Psi_i | H | P \psi_j \rangle \quad (10)$$

The quantities, such as the Kohn–Sham Hamiltonian of the dimer H and $\Psi_{i(j)}$ of hole/electron transport in the monomer, were calculated using the CATNIP program.^{30,31}

3. RESULTS AND DISCUSSION

The calculated geometric parameters of the furan/thiophene-substituted derivatives are given in Table 2. BPTFT retains its planar backbone from BP3T, and for all other systems, the values vary with respect to the level of furan substitution in the system. When two or more furan rings are present in the system, they influence the molecular dihedral angle. Both BP3F and BPFTF have angles of about 117°. Interestingly, the dihedral angles of BPFFT and BPFTT are exactly same at about 120.96°. The calculated bond lengths, bond distances, and bond length alteration (BLA) values are given in the Supporting Information (Section 1). It can be seen that with an increase in the number of furan rings, the BLA values decreased from 0.08 to 0.03, and BP3F shows the lowest values, indicating the highest π conjugation in the system. Also, the cationic and anionic forms of the system have lower BLA values than their neutral forms, indicating that the charged systems have more efficient conjugation than the neutral ones.

Table 2. Calculated Geometrical Parameters of the BPFT System^a

system	A1 = A2	B1 = B2	C1 = C2	P–X–P	$\langle \cos^2 \phi \rangle$
BP3T	1.464	1.443	120.50	159.00	0.136
BPFTT	1.451	1.431	120.96	159.03	0.137
BPTFT	1.463	1.437	121.43	173.62	0.453
BPFFT	1.451	1.431	120.96	159.03	0.137
BPFTF	1.453	1.437	117.29	138.26	0.999
BP3F	1.453	1.432	117.31	164.24	0.408

^aA1 and A2 are bond lengths between the phenylene and the thiophene/furan rings. B1 and B2 are bond lengths between the thiophene/furan rings. C1 and C2 are bond angles between the phenylene and the thiophene/furan rings. P–X–P is the dihedral angle with respect to the central ring. $\langle \cos^2 \phi \rangle$ is the degree of backbone twisting.

To explicitly extract the molecular planarity, we measured the bond angles and bond lengths between the phenyl rings and the center molecules (independent of whether furan or thiophene). BPTFT shows the highest planarity followed by BP3F, BPFTT, and BPFFT. In the case of dihedral angles, up to 0.72° variation has been observed (Table 2). BPFTT and BPFFT show the highest and BP3F shows the lowest ϕ value, indicating a decrease of the planarity in the BP3F system. A similar trend is observed in the case of the anionic and cationic forms of the system. However, the only variation observed is that the anionic form is more planar than that of the cationic form.

Since the planarity and backbone twisting of the system are crucial requirements to understand the functionality of the

system, we have calculated the degree of backbone twisting by estimating the $\langle \cos^2 \phi \rangle$ values.³² This value is a better predictor of backbone twisting than the usual lowest energy dihedral angles due to the fact that the twisted molecule could be statistically more planar than the optimized state. The value can be calculated using the equation

$$\langle \cos^2 \phi \rangle = \int_0^{2\pi} P(\pi) \cos^2 \phi \, d\phi / \int_0^{2\pi} P(\pi) \, d\phi \quad (11)$$

where $\langle \cos^2 \phi \rangle$ is an empirical parameter to represent the planarity and orbital overlap, $P(\pi)$ is the probability distribution calculated from the Boltzmann equation, and ϕ ranges from 0° to 180° (for s-trans and s-cis conformations), and the corresponding values are given in Table 2.

Considering the case of BPFTF, the dihedral angle values are about 6.353° , showing the planar nature of the system. On the other hand, low $\langle \cos^2 \phi \rangle$ values indicate that there is a higher degree of rotational disorder along the conjugated backbone in the system. Similarly, the lower $\langle \cos^2 \phi \rangle$ values of BPFTT and BPFFT indicate the smaller repulsion between the moieties in the system, whereas in the case of BPFTF, attractive noncovalent interactions contributed to the planarity of the system. For BPTFT, the variation with respect to BP3F and BP3T is due to the increase in conjugation length leading to more resonance stabilization.

In the case of BP3F, since furan has higher aromaticity than the thiophene moiety, its planar conformation and backbone planarization have been minimized.

The calculated frontier molecular orbitals and energy gap of the systems are given in Figure 2. The pristine BP3T system

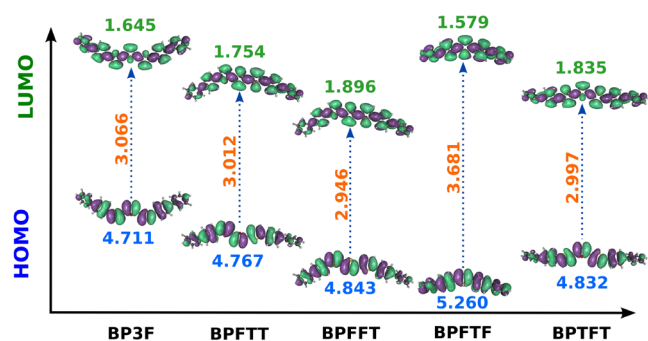


Figure 2. Electronic properties.

has a HOMO value of about 4.912 eV, LUMO value of about 1.989 eV, and energy gap of about 2.92 eV.²⁴ In all cases, in both the HOMO and the LUMO the electron density is distributed to the entire system. However, major localization and delocalization can be observed in the thiophene and furan rings of the systems. The charge distribution over the entire system can be attributed to the high degeneracy of the

molecular orbitals, and it is advantageous in the case of the charge mobility of the system.^{33,34} The band gaps of the systems vary with respect to the furan substitution. BPFTF has the highest energy gap of 3.681 eV, and BPFFT has the lowest value of about 2.946 eV. It can be seen that the higher the $\langle \cos^2 \phi \rangle$ values, the higher the band gap values. An increase in LUMO and decrease in the HOMO is a common trend expected in any conjugation system due to the weak bonding and antibonding on the inter ring bond.³²

Electron affinity (EA) and ionization potential (IP) values can be used to represent the oxidation and reduction capabilities of a molecule.^{35,36} In the present work, these values for the BPFT systems were calculated using the following relations

$$IP = E_{\text{cation}} - E_{\text{neutral}}$$

$$EA = E_{\text{neutral}} - E_{\text{anion}}$$

where E_{neutral} , E_{cation} , and E_{anion} are the energies of the neutral, cationic, and anionic forms of the each molecular system, and the corresponding calculated values are given in Table 3. Considering the OLET device architecture, the electron affinity can be related to the air stability of the system and the ionization potential can be related to the hole injection.^{37,38} Often for a p-type system lower IP values are expected.³⁹ It can be seen that with the substitution of the furan rings it would be hard to achieve an ambipolar nature in the system. In particular, BP3F shows smaller IP values compared to the other systems with the thiophene rings. On the other hand, the EA values decrease with an increase in the number of furan rings, indicating the air-stable nature of these molecules.

Computed reorganization energy (λ) values are given in Table 3, and these values could be used to understand the charge transfer in the system by the electronic coupling between the adjacent molecules.^{40,41} In crystalline structures, these values can be used to estimate the geometry relaxation and electron–phonon coupling. λ values are inversely proportional to the mobility of the system. Thus, systems like BP3F have higher mobility values than other systems. For most of the systems the hole reorganization values are one order higher than the electron reorganization energies. Further, the increase in reorganization energy values are in line with the increase of nonplanarity in the molecular systems. The charge transfer integral (CTI) values of the systems were calculated using cofacial dimers, and the corresponding values are given in Table 3. Since planar structures are more favorable to use in an OLET device, we performed only the vertical charge transitions and excluded the tilt angle measurements. In such a case, a zero net polarization would result due to the face-to-face orientation. However, due to molecular twisting there is slightly distorted stacking. From the obtained values (Table 3) it can be seen that the values increase with the incorporation of

Table 3. Calculated Electronic and Charge Transfer Properties of the System

system	IP	EA	J_{eff}	λ_{hole}	λ_{elec}	μ_{hole}	μ_{elec}
BP3F	0.0045	0.0229	-0.644	8.72	0.95	5.4700	0.8830
BPFTT	0.3212	0.0620	-1.198	43.6	2.31	0.1922	0.0076
BPFFT	0.4227	0.1582	-1.325	82.8	2.75	1.8239	0.0111
BPFTF	0.2151	0.0282	-0.815	4.36	1.83	0.8892	0.0029
BPTFT	0.2173	0.0306	-1.267	4.36	0.78	2.1483	1.3156
BP3T	5.9705	1.1510	-0.016	0.10	0.96	0.8122	0.1702

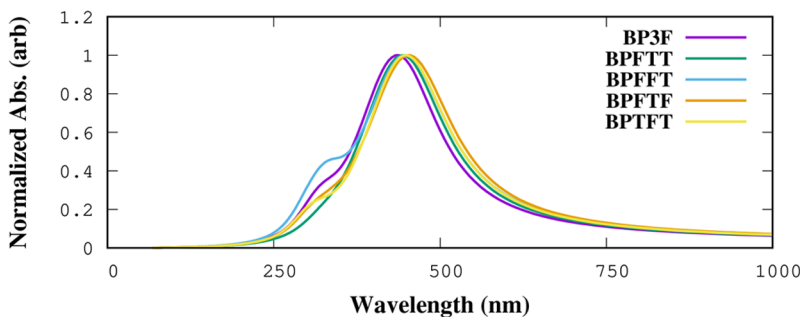


Figure 3. Absorption spectrum of pristine and furan-substituted BPFT systems.

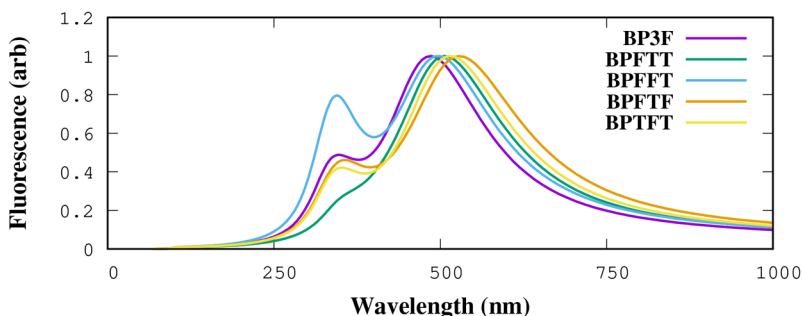


Figure 4. Emission spectrum of pristine and furan-substituted BPFT systems.

furan, and BP3F shows the highest CTI values. The reorganization energy and CTI values are used to calculate the charge transfer mobility of the system (Table 3). All of the systems exhibit a hole transfer mobility that is one order of magnitude higher than the electron transfer mobility. Also, in both cases, BPFTT shows the lowest mobility values among other furan-substituted systems.

The absorption spectra of the BPFT systems are given in Figure 3. The spectra are similar to our previous report on the BP3T system with a shoulder peak around 300 nm and a major absorption peak around 480 nm. Interestingly, in our previous study, we observed a reasonable red shift with respect to the number of thiophene rings in the BPT system.²⁴ However, in the present study, even though a slight variation in the shoulder peak has been observed, the spectra are consistent for the different systems. This can be understood from the frontier molecular orbitals. Since the charge delocalization is almost the same for all of the systems, similar optical properties have been observed. However, the slight variation in the shoulder peaks could be attributed to the planarity of the system.²⁴ Lower $\langle \cos^2 \phi \rangle$ values slightly increase the absorption in the shoulder peak region. The simulated emission spectra are shown in Figure 4, and the corresponding oscillator strengths (f_{osc}) are given in Table 4.

Table 4. Calculated Optical Parameters of Pristine and Furan-Substituted BPFT Systems

system	E (cm ⁻¹)	f_{osc}	τ (μs)	TDM (au ²)
BP3F	23053.3	2.581 8	1.092	36.869
BPFTT	20423.8	2.988 4	1.202	48.170
BPFFT	19516.7	3.144 7	1.251	53.045
BPFTF	22407.1	2.443 8	1.221	35.905
BPTFT	22275.1	2.758 1	1.095	40.764
BP3T	19492.0	2.393 1	1.648	40.419

The emission peaks are assigned to $\pi \rightarrow \pi^*$ transitions arising from LUMO \rightarrow HOMO transitions. In all of the systems, the major emission is a $S_1 \rightarrow S_0$ transition, and tweaking the photoluminescence quantum yield (PLQY) can be done by modifying this transition. Using the energy gap and f_{osc} values, we calculated the exciton binding energy values, and they are in the order of BP3F < BPFTT, indicating the higher exciton binding energies for more than one thiophene ring-substituted systems. Thus, it is easy to destroy an electron–hole pair with more furan rings, and a higher emission is possible in these systems.

In optoelectronic systems, radiative lifetime values could be used to estimate the emission efficiency of the system. It can be calculated using the relation

$$\tau = \frac{1.499}{f_{osc} E^2}$$

where E is the excitation energy, and the corresponding calculated values are given in Table 4. Almost similar values indicate the strong emissive nature in all of the systems. However, the decreasing τ values of the BPFT systems with respect to the pristine system can be attributed to the molecular planarity. It can be further explored using the transition dipole moment calculations (see Supporting Information section 3). Since the maximum efficiency can be obtained with the perfect alignment of the dimers, in the present work, TDM calculations were carried out along with vibrational analysis, and the obtained spectra are given in Figure 5.^{42,43} The corresponding data can be obtained from the Supporting Information (section 2). Similar to the absorption and emission spectra, the vibrational spectrum of the system is in accordance with the BP3T results. A note of warning is that in the present case we have considered only the molecular aspect of the furan substitution in the biphenyl/thiophene system. However, experimental realization of the

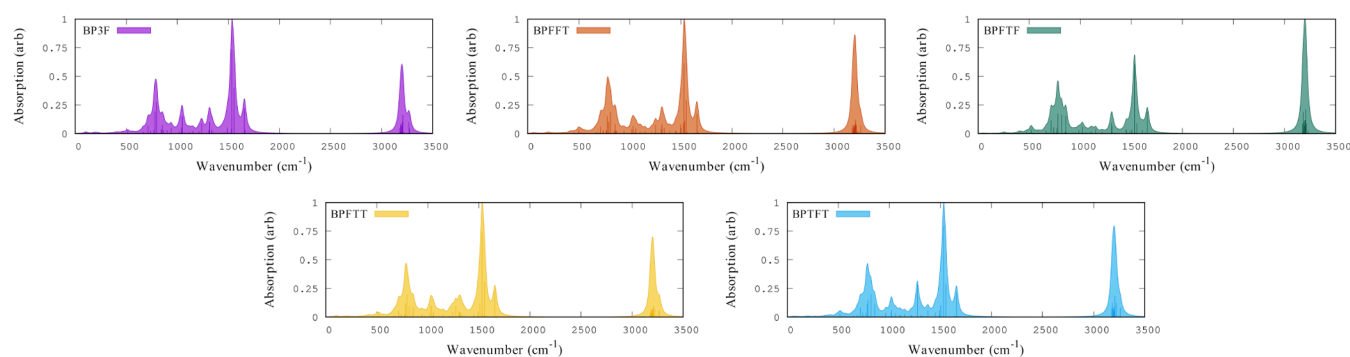


Figure 5. Vibrational frequencies and transition dipole moments of BPFT systems.

same material could be affected by a multitude of factors ranging from crystal/thin film growth to the device fabrication and characterization methods. Thus, the significance of the reported data is that it could act as a potential starting point for the fabrication of prototypes and allow one to easily explore the role of intermolecular forces in such devices.

Finally, in order to compare all of the results, we formulated an empirical entity (O_{eff}) which is the ratio between the product of the mobilities and $\langle \cos^2 \phi \rangle$ and the product of TDM and $\langle \cos^2 \phi \rangle$. This entity is derived from the fact that the ambipolar charge transfer and the transition dipole moment are related to the planarity of the molecular system, and these values could be used as an estimation for the efficiency of a molecular system for organic light-emitting transistors. The obtained values are given in the Supporting Information (section 4) and depicted in Figure 6. Compared to pristine

transport result in lower O_{eff} values for the BPFTT and BPFFT systems.

4. CONCLUSION

Furan-substituted biphenyl/thiophenes were optimized using density functional theory with the B3LYP functional and 6-311G(d,p) basis set. It was found that with the substitution of furan rings the molecular planarity significantly varies. Thus, variation in the optoelectronic properties of the system has been observed. In terms of the electronic distribution, we observed that for all of the molecules the HOMO and LUMO were evenly distributed to the molecule, independent of the molecular substitution. On the other hand, substitution altered the energy gap between the HOMO and the LUMO, and they are in the range between 2.946 and 3.681. The charge transfer integral of the system decreases with respect to the number of furan rings, whereas the reorganization energy greatly depends on the molecular planarity. With the substitution of furan, the electron mobility is reduced by one fold whereas the hole mobility is greatly improved. This along with the lower IP value indicates the high atmospheric stability of this material. In the case of the optical properties, furan substitution does not greatly alter the absorption region of BP3T, and the corresponding oscillator strengths are also similar to the pristine system. However, the transition dipole moments significantly varied, and the systems with either double furan or double thiophene substitution show higher values. The radiative lifetime values decrease with a decrease in the molecular rotational disorder, i.e., the more planar the molecule the higher its τ values. The empirical entity O_{eff} values of the BPFT systems show that BP3F has the highest value followed by BPTFT. Surprisingly, BPFTT, BPFFT, and BPFTF are lower performing than the pristine BP3T system due to the higher $\langle \cos^2 \phi \rangle$ values. In summary, the results confirm the potential of complete furan substitution in the BP3T system. However, considering the effectiveness toward OLETs, selected area substitution like BPTFT in the present case could be the optimal choice for real-life applications.

■ ASSOCIATED CONTENT

SI Supporting Information

The Supporting Information is available free of charge at <https://pubs.acs.org/doi/10.1021/acs.jpca.1c09977>.

Optimized geometries, vibrational spectra, transition dipole moments, and empirical calculation details ([PDF](#))

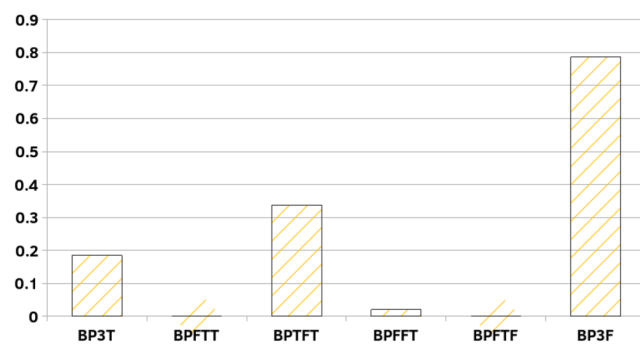


Figure 6. Comparison of all of the derivatives used in the present study.

BP3T, a system with all furan moieties, BP3F has the highest O_{eff} values. This is mainly due to the higher hole transfer mobility and the lower degree of rotational disorder in the system. This was followed by BPTFT, with values between BP3T and BP3F. In this case too, reasonable mobility with lower nonplanarity contributes to the better O_{eff} values. It is worth noting that BPTFT is the system with the highest electron mobility in the present study. These materials could be a better choice than BP3F, where the material's ambipolar transport really matters. Also, BPFTT, BPFFT, and BPFTF have lower O_{eff} values than the other three systems. In the case of BPFTF, a very strong rotational disorder highly limits these molecules for the consideration of OLETs. On the other hand, even with higher TDM values, lower values of carrier charge

AUTHOR INFORMATION

Corresponding Authors

Periyasamy Angamuthu Praveen – *Organic Optoelectronics Research Laboratory, Department of Physics, Indian Institute of Science Education and Research (IISER), Tirupati 517 507 Andhra Pradesh, India; Email: praveen@iisertirupati.ac.in*

Thangavel Kanagasekaran – *Organic Optoelectronics Research Laboratory, Department of Physics, Indian Institute of Science Education and Research (IISER), Tirupati 517 507 Andhra Pradesh, India; orcid.org/0000-0003-3675-2434; Email: kanagasekaran@iisertirupati.ac.in*

Authors

Perumal Muthuraja – *Department of Chemistry, Indian Institute of Science Education and Research (IISER), Tirupati 517 507 Andhra Pradesh, India*

Purushothaman Gopinath – *Department of Chemistry, Indian Institute of Science Education and Research (IISER), Tirupati 517 507 Andhra Pradesh, India; orcid.org/0000-0003-4673-2816*

Complete contact information is available at:

<https://pubs.acs.org/10.1021/acs.jpca.1c09977>

Notes

The authors declare no competing financial interest.

ACKNOWLEDGMENTS

P.A.P. and P.M. acknowledge financial support from the Indian Institute of Science Education and Research (IISER), Tirupati.

REFERENCES

- (1) Ji, L.; Shi, J.; Wei, J.; Yu, T.; Huang, W. Air-Stable Organic Radicals: New-Generation Materials for Flexible Electronics? *Adv. Mater.* **2020**, *32*, 1908015.
- (2) Dauzon, E.; Sallenave, X.; Plesse, C.; Goubard, F.; Amassian, A.; Anthopoulos, T. D. Pushing the Limits of Flexibility and Stretchability of Solar Cells: A Review. *Adv. Mater.* **2021**, *33*, 2101469.
- (3) Ponnappa, S. P.; Liu, Q.; Umer, M.; MacLeod, J.; Jickson, J.; Ayoko, G.; Shiddiky, M. J.; O'Mullane, A. P.; Sonar, P. Naphthalene flanked diketopyrrolopyrrole: a new conjugated building block with hexyl or octyl alkyl side chains for electropolymerization studies and its biosensor applications. *Polym. Chem.* **2019**, *10*, 3722–3739.
- (4) Ling, H.; Liu, S.; Zheng, Z.; Yan, F. Organic flexible electronics. *Small Methods* **2018**, *2*, 1800070.
- (5) Moser, M.; Wadsworth, A.; Gasparini, N.; McCulloch, I. Challenges to the Success of Commercial Organic Photovoltaic Products. *Adv. Energy Mater.* **2021**, *11*, 2100056.
- (6) Yang, H.; Lee, J.; Cheong, J. Y.; Wang, Y.; Duan, G.; Hou, H.; Jiang, S.; Kim, I.-D. Molecular engineering of carbonyl organic electrodes for rechargeable metal-ion batteries: fundamentals, recent advances, and challenges. *Energy Environ. Sci.* **2021**, *14*, 4228–4267.
- (7) Mohajeri, A.; Omidvar, A.; Setoodeh, H. Fine structural tuning of thieno [3, 2-b] pyrrole donor for designing banana-shaped semiconductors relevant to organic field effect transistors. *J. Chem. Inf. Model.* **2019**, *59*, 1930–1945.
- (8) Wang, Y.; Hao, W.; Huang, W.; Zhao, H.; Zhu, J.; Fang, W. Tuning the Ambipolar Character of Copolymers with Substituents: A Density Functional Theory Study. *J. Phys. Chem. Lett.* **2020**, *11*, 3928–3933.
- (9) Wang, L.; Dai, J.; Song, Y. The impact of diperfluorophenyl and thiényl substituents on the electronic structures and charge transport properties of the fused thiophene semiconductors. *Int. J. Quantum Chem.* **2019**, *119*, No. e25824.
- (10) Hecht, M.; Würthner, F. Supramolecularly engineered J-aggregates based on perylene bisimide dyes. *Acc. Chem. Res.* **2021**, *54*, 642–653.
- (11) Kim, J.; Batagoda, T.; Lee, J.; Sylvinson, D.; Ding, K.; Saris, P. J.; Kaipa, U.; Oswald, I. W.; Omary, M. A.; Thompson, M. E.; et al. Systematic Control of the Orientation of Organic Phosphorescent Pt Complexes in Thin Films for Increased Optical Outcoupling. *Adv. Mater.* **2019**, *31*, 1900921.
- (12) Demchenko, A. P. Excitons in carbonic nanostructures. *C* **2019**, *5*, 71.
- (13) Zheng, C.; Mark, M. F.; Wiegand, T.; Diaz, S. A.; Cody, J.; Spano, F. C.; McCamant, D. W.; Collison, C. J. Measurement and theoretical interpretation of exciton diffusion as a function of intermolecular separation for squaraines targeted for bulk heterojunction solar cells. *J. Phys. Chem. C* **2020**, *124*, 4032–4043.
- (14) Chaudhry, M. U.; Muhieddine, K.; Wawrzinek, R.; Sobus, J.; Tandy, K.; Lo, S.-C.; Namdas, E. B. Organic light-emitting transistors: advances and perspectives. *Adv. Funct. Mater.* **2020**, *30*, 1905282.
- (15) Wan, Y.; Deng, J.; Wu, W.; Zhou, J.; Niu, Q.; Li, H.; Yu, H.; Gu, C.; Ma, Y. Efficient Organic Light-Emitting Transistors Based on High-Quality Ambipolar Single Crystals. *ACS Appl. Mater. Interfaces* **2020**, *12*, 43976–43983.
- (16) Ma, S.; Zhou, K.; Hu, M.; Li, Q.; Liu, Y.; Zhang, H.; Jing, J.; Dong, H.; Xu, B.; Hu, W.; et al. Integrating Efficient Optical Gain in High-Mobility Organic Semiconductors for Multifunctional Optoelectronic Applications. *Adv. Funct. Mater.* **2018**, *28*, 1802454.
- (17) Dokiya, S.; Ishigami, H.; Akazawa, T.; Sasaki, F.; Yanagi, H. Organic light-emitting diodes with a PIN structure of only thiophene/phenylene co-oligomer derivatives. *Jpn. J. Appl. Phys.* **2020**, *59*, 041004.
- (18) Liu, L.; Cai, C.; Zhang, Z.; Zhang, S.; Deng, J.; Yang, B.; Gu, C.; Ma, Y. Lamellar Organic Light-Emitting Crystals Exhibiting Spectral Gain and 3.6% External Quantum Efficiency in Transistors. *ACS Materials Letters* **2021**, *3*, 428–432.
- (19) Qin, Z.; Gao, H.; Dong, H.; Hu, W. Organic Light-Emitting Transistors Entering a New Development Stage. *Adv. Mater.* **2021**, *33*, 2007149.
- (20) Sosorev, A. Y.; Trukhanov, V. A.; Maslenikov, D. R.; Borshchev, O. V.; Polyakov, R. A.; Skorotetcky, M. S.; Surin, N. M.; Kazantsev, M. S.; Dominiskiy, D. I.; Tafeenko, V. A.; et al. Fluorinated Thiophene-Phenylene Co-Oligomers for Optoelectronic Devices. *ACS Appl. Mater. Interfaces* **2020**, *12*, 9507–9519.
- (21) Shang, H.; Shimotani, H.; Kanagasekaran, T.; Tanigaki, K. Separation in the Roles of Carrier Transport and Light Emission in Light-Emitting Organic Transistors with a Bilayer Configuration. *ACS Appl. Mater. Interfaces* **2019**, *11*, 20200–20204.
- (22) Kanagasekaran, T.; Shimotani, H.; Shimizu, R.; Hitosugi, T.; Tanigaki, K. A new electrode design for ambipolar injection in organic semiconductors. *Nat. Commun.* **2017**, *8*, 999.
- (23) Shang, H.; Shimotani, H.; Ikeda, S.; Kanagasekaran, T.; Oniwa, K.; Jin, T.; Asao, N.; Yamamoto, Y.; Tamura, H.; Abe, K.; et al. Comparative Study of Single and Dual Gain-Narrowed Emission in Thiophene/Furan/Phenylene Co-Oligomer Single Crystals. *J. Phys. Chem. C* **2017**, *121*, 2364–2368.
- (24) Praveen, P. A.; Bhattacharya, A.; Kanagasekaran, T. A DFT study on the electronic and photophysical properties of biphenyl/thiophene derivatives for organic light emitting transistors. *Materials Today Communications* **2020**, *25*, 101509.
- (25) Cicoria, F.; Santato, C. Organic light emitting field effect transistors: advances and perspectives. *Adv. Funct. Mater.* **2007**, *17*, 3421–3434.
- (26) Turan, H. T.; Yavuz, I.; Aviyente, V. Understanding the Impact of Thiophene/Furan Substitution on Intrinsic Charge-Carrier Mobility. *J. Phys. Chem. C* **2017**, *121*, 25682–25690.
- (27) Koskin, I. P.; Mostovich, E. A.; Benassi, E.; Kazantsev, M. S. Way to highly emissive materials: Increase of rigidity by introduction of a furan moiety in co-oligomers. *J. Phys. Chem. C* **2017**, *121*, 23359–23369.

- (28) Zheng, B.; Huo, L. Recent Advances of Furan and Its Derivatives Based Semiconductor Materials for Organic Photovoltaics. *Small Methods* **2021**, *5*, 2100493.
- (29) Derrida, B. Velocity and diffusion constant of a periodic one-dimensional hopping model. *J. Stat. Phys.* **1983**, *31*, 433–450.
- (30) Valeev, E. F.; Coropceanu, V.; da Silva Filho, D. A.; Salman, S.; Brédas, J.-L. Effect of electronic polarization on charge-transport parameters in molecular organic semiconductors. *J. Am. Chem. Soc.* **2006**, *128*, 9882–9886.
- (31) Baumeier, B.; Kirkpatrick, J.; Andrienko, D. Density-functional based determination of intermolecular charge transfer properties for large-scale morphologies. *Phys. Chem. Chem. Phys.* **2010**, *12*, 11103–11113.
- (32) Che, Y.; Perepichka, D. F. Quantifying Planarity in the Design of Organic Electronic Materials. *Angew. Chem., Int. Ed.* **2021**, *60*, 1364–1373.
- (33) Moliton, A.; Hiorns, R. C. Review of electronic and optical properties of semiconducting π -conjugated polymers: applications in optoelectronics. *Polym. Int.* **2004**, *53*, 1397–1412.
- (34) Yamaguchi, Y.; Takubo, M.; Ogawa, K.; Nakayama, K.-i.; Koganezawa, T.; Katagiri, H. Terazulene isomers: polarity change of OFETs through molecular orbital distribution contrast. *J. Am. Chem. Soc.* **2016**, *138*, 11335–11343.
- (35) Ullah, H.; Ayub, K.; Ullah, Z.; Hanif, M.; Nawaz, R.; Bilal, S.; et al. Theoretical insight of polypyrrole ammonia gas sensor. *Synth. Met.* **2013**, *172*, 14–20.
- (36) Martinez, A.; Vargas, R.; Galano, A. What is important to prevent oxidative stress? A theoretical study on electron-transfer reactions between carotenoids and free radicals. *J. Phys. Chem. B* **2009**, *113*, 12113–12120.
- (37) Takenobu, T.; Takano, T.; Shiraishi, M.; Murakami, Y.; Ata, M.; Kataura, H.; Achiba, Y.; Iwasa, Y. Stable and controlled amphoteric doping by encapsulation of organic molecules inside carbon nanotubes. *Nat. Mater.* **2003**, *2*, 683–688.
- (38) Choulis, S. A.; Choong, V.-E.; Patwardhan, A.; Mathai, M. K.; So, F. Interface Modification to Improve Hole-Injection Properties in Organic Electronic Devices. *Adv. Funct. Mater.* **2006**, *16*, 1075–1080.
- (39) Liu, C.-C.; Mao, S.-W.; Kuo, M.-Y. Cyanated Pentaceno[2,3-c]chalcogenophenes for Potential Application in Air-Stable Ambipolar Organic Thin-Film Transistors. *J. Phys. Chem. C* **2010**, *114*, 22316–22321.
- (40) Wadsworth, A.; Chen, H.; Thorley, K. J.; Cendra, C.; Nikolka, M.; Bristow, H.; Moser, M.; Salleo, A.; Anthopoulos, T. D.; Sirringhaus, H.; et al. Modification of Indacenodithiophene-Based Polymers and its Impact on Charge Carrier Mobility in Organic Thin-Film Transistors. *J. Am. Chem. Soc.* **2020**, *142*, 652–664.
- (41) Risko, C.; Kushto, G. P.; Kafati, Z. H.; Brédas, J. L. Electronic properties of silole-based organic semiconductors. *J. Chem. Phys.* **2004**, *121*, 9031–9038.
- (42) Chuang, C.; Bennett, D. I.; Caram, J. R.; Aspuru-Guzik, A.; Bawendi, M. G.; Cao, J. Generalized kasha's model: T-dependent spectroscopy reveals short-range structures of 2d excitonic systems. *Chem.* **2019**, *5*, 3135–3150.
- (43) Yu, H.; Aziz, H. Exciton-Induced Degradation of Hole Transport Layers and Its Effect on the Efficiency and Stability of Phosphorescent Organic Light-Emitting Devices. *Advanced Optical Materials* **2019**, *7*, 1800923.

□ Recommended by ACS

Roles of Molecular Spatial Arrangement in Exciton Energy Transfer in Organic Light-Emitting Diodes: A Theoretical Study

Xin Jiang, Wei Shen, et al.

MARCH 20, 2023

THE JOURNAL OF PHYSICAL CHEMISTRY C

READ ▶

Self-Assembled Oligothiophenes for Photocatalytic Hydrogen Production and Simultaneous Organic Transformation

Bramhaiah Kommula, Santanu Bhattacharyya, et al.

SEPTEMBER 26, 2022

ACS APPLIED NANO MATERIALS

READ ▶

Syntheses of Thiophene and Thiazole-Based Building Blocks and Their Utilization in the Syntheses of A-D-A Type Organic Semiconducting Materials with Dithienosilolo Ce...

Tomi A. O. Parviainen, Juha P. Heiskanen, et al.

JULY 21, 2022

ACS OMEGA

READ ▶

Nonpolymer Organic Solar Cells: Microscopic Phonon Control to Suppress Nonradiative Voltage Loss via Charge-Separated State

Takaaki Nagatomo, Yasuhiro Kobori, et al.

DECEMBER 30, 2022

ACS PHYSICAL CHEMISTRY AU

READ ▶

Get More Suggestions >